



Full length article

Molecular cloning and expression analysis of *MyD88* and *TRAF6* in Qihe crucian carp *Carassius auratus*Jie Zhang^a, Yachen Zhu^a, Zhuo Chen^b, Chunjing Li^a, Xianliang Zhao^a, Xianghui Kong^{a,*}^a College of Fisheries, Henan Normal University, Xinxiang, 453007, PR China^b College of Life Science, Henan Normal University, Xinxiang, 453007, PR China

ARTICLE INFO

Keywords:

Myeloid differentiation factor 88
Tumor necrosis factor receptor-associated factor 6
Carassius auratus
Aeromonas hydrophila

ABSTRACT

Myeloid differentiation factor 88 (MyD88) and tumor necrosis factor receptor-associated factor 6 (TRAF6) are two critical signal transducers in toll-like receptor (TLR) pathway. In the present study, we identified and characterized the homologues of *MyD88* and *TRAF6* in Qihe crucian carp *Carassius auratus*, termed as *CaMyD88* and *CaTRAF6*, respectively, and examined their roles during pathogenic infection. Full-length cDNA of *CaMyD88* was 2463 bp, including a 191 bp 5'-untranslated region (UTR), a 1417 bp 3'-UTR, and an 855 bp open reading frame (ORF) encoding for a putative protein with 284 amino acids. Full-length cDNA of *CaTRAF6* was identified to be 2555 bp, consisting of a 52 bp 5'-UTR, an 871 bp 3'-UTR, and a 1632 bp ORF encoding a protein of 543 amino acids. Deduced amino acid sequences of *CaMyD88* and *CaTRAF6* contained the typical domains (*CaMyD88*: death domain and TIR domain; *CaTRAF6*: one RING-type zinc finger domain, two TRAF-type zinc finger domains, one coiled-coil region, and one conserved C-terminal meprin and TRAF homology domain) as in other fish. Quantitative Real-Time PCR (qRT-PCR) analysis revealed that both *CaMyD88* and *CaTRAF6* were ubiquitously expressed throughout the development stages and appeared to be developmentally regulated. In addition, *CaMyD88* and *CaTRAF6* had a broadly distribution of expression in all examined eleven tissues of healthy fish, although the transcript levels varied among the different tissues. Moreover, it was found that mRNA expressions of *CaMyD88* and *CaTRAF6* were generally up-regulated after stimulation by polyI:C, flagellin, and *Aeromonas hydrophila* in spite of the down-regulation appeared at some time points or tissues. These results indicated that *CaMyD88* and *CaTRAF6* play the critical roles in the immune defense of Qihe crucian carp against pathogenic invasion. The present findings will provide the valuable information for understanding the innate immune responses of Qihe crucian carp and contribute to develop the preventive way against pathogens.

1. Introduction

The innate immune system is the most ancient and universal form of host defense in animals, and plays a central role in immune response against pathogen invasion [1]. It is triggered by germline-encoded pattern recognition receptors (PRRs) which are conserved in invertebrate and vertebrate lineages and responsible for sensing the conserved molecular structure of pathogens, known as pathogen-associated molecular patterns (PAMPs) [2,3]. As the first and best characterized pattern recognition receptors (PRRs), toll-like receptors (TLRs) recognize the PAMPs such as lipopolysaccharide (LPS), peptidoglycan (PGN), flagellin, DNA containing unmethylated CpG motifs (CpG DNA), lipopeptides, and polyinosinic:polycytidylic acid (polyI:C), etc. and trigger the signaling pathways that activate immune cells in response to pathogen infection via recruiting the different adaptor

proteins [3–5]. The TLR signaling pathways are largely classified into myeloid differentiation factor 88 (MyD88)-dependent and MyD88-independent pathway [1]. MyD88 and tumor necrosis factor receptor-associated factor 6 (TRAF6) are two of the critical signal transducers in the MyD88-dependent pathway [5].

MyD88, as the first identified TIR domain containing adaptor protein, was recruited by all TLRs except TLR3 in mammals [6]. Principal functional domains of MyD88 consisted of C-terminal Toll-like/IL-1 receptor (TIR) domain and N-terminal death domain [7]. The TIR domain interacted with the TIR domain of activated TLRs, and the death domain was involved in recruiting downstream molecule IL-1 receptor-associated protein kinases (IRAKs) [8]. Subsequently, the MyD88-IRAK complex induced the auto-ubiquitination of tumor necrosis factor receptor-associated factor 6 (TRAF6), the only member of TRAFs family that participates in the MyD88-dependent pathway [9,10]. Then, the

* Corresponding author. No. 46, Jianshe Road, College of Fisheries, Henan Normal University, Xinxiang, 453007, PR China.

E-mail address: xhkong@htu.cn (X. Kong).<https://doi.org/10.1016/j.fsi.2019.02.034>

Received 18 December 2018; Received in revised form 11 February 2019; Accepted 15 February 2019

Available online 18 February 2019

1050-4648/© 2019 Elsevier Ltd. All rights reserved.

nuclear factor κ B (NF- κ B) and activator protein (AP-1) were activated, and led to the production of pro-inflammatory cytokines and eventually to eliminate pathogens [5]. MyD88 and/or TRAF6 have been identified in several teleost species, such as orange-spotted grouper (*Epinephelus coioides*) [11,12], common carp (*Cyprinus carpio*) [13], grass carp (*Ctenopharyngodon idella*) [14,15], blunt snout bream (*Megalobrama amblycephala*) [16], Japanese eel (*Anguilla japonica*) [17], silvery pomfret (*Pampus argenteus*) [18], and black carp (*Mylopharyngodon piceus*) [19]. These studies provided valuable information for understanding the molecular characteristics and functions of MyD88 and/or TRAF6 in fish.

Qihe crucian carp (*Carassius auratus*), an endemic triploid freshwater fish with natural gynogenesis, is one of the most commercially important fish and has been widely cultured throughout the north of Henan Province, China [20]. However, in recent years, the high density and intensive farming has resulted in the weaker immunity and outbreak of fish diseases, which causes extensive losses in aquaculture. We have found that TLR5 and TLR22 played the important roles in the immune response of Qihe crucian carp against pathogenic invasion [21,22]. MyD88 and TRAF6 were the critical signal transduction proteins in TLR5/22 pathways [5]. However, MyD88 and TRAF6 have not been identified in Qihe crucian carp, and their functions are still unclear. Therefore, in order to further understand the mechanism underlying the immune responses during infection and develop preventive and therapeutic measures against pathogens, in the present study, *MyD88* and *TRAF6* were cloned and characterized in Qihe crucian carp (designated as *CaMyD88* and *CaTRAF6*), and tissue distribution, expression levels during embryonic development, transcription responses in different tissues were investigated after challenges of *Aeromonas hydrophila*, flagellin, and polyI:C. The aims of this study were to determine the structures, functions, and expressions of *CaMyD88* and *CaTRAF6* in Qihe crucian carp respectively, and to reveal the process and mechanism of immune responses involved in MyD88-dependent pathway against pathogen infection in Qihe crucian carp.

2. Materials and methods

2.1. Fish, immune challenge and sample collection

Healthy fish were purchased from the original breeding farm of Qihe crucian carp in Henan Province. Fish with an average body weight of 35 ± 5 g were acclimated to laboratory conditions for two weeks in aerated freshwater at 25 ± 2 °C and were fed twice daily with commercial feed until 24 h before the treatment.

The immune challenge was performed according to the method as described previously [22]. In brief, experimental fish were randomly divided into one control group and three treatment groups (20 fish per group). As treatment groups, fish were injected intraperitoneally with 200 μ L polyI:C (Sigma, USA) (0.2 mg/mL), flagellin (*Salmonella typhimurium* strain 14028, Sigma, USA) (2 μ g/mL), and *A. hydrophila* suspension (5×10^7 CFU/mL), respectively. Fish injected with 200 μ L 0.65% physiological saline were used as the control group. After 3, 6, 12, 24, and 48 h post infection (hpi), four tissues (gill, liver, spleen, and head kidney) from each fish were collected, respectively, and immediately stored at -80 °C until RNA extraction. Three fish were sampled from each group at each time point, and the experiments were performed in triplicate.

To investigate expression patterns during the early development, embryos at eight embryonic stages (fertilized egg, cleavage, blastula, gastrula, neurula, tail-bud, heart-beating, and hatching stage) and larvae [1, 5, 10, 20, and 30 d post hatching (dph)] were collected respectively. The different embryonic stages for samples were identified microscopically. To profile expression difference in different tissues, eleven tissues (gill, head kidney, trunk kidney, spleen, liver, intestine, heart, skin, muscle, brain, and blood) were excised from healthy fish. All the samples were immediately stored at -80 °C until RNA

extraction.

2.2. DNA and RNA isolation, cDNA synthesis

Genomic DNA was isolated in muscle of Qihe crucian carp using the classical phenol-chloroform procedure followed by ethanol precipitation [23]. Total RNA was isolated using RNAiso Plus (TaKaRa, Japan) according to the manufacturer's instructions. RNA integrity and concentrations were determined by electrophoresis on 1% agarose gel and NanoDrop 2000 spectrophotometer (Thermo Scientific, USA), respectively. First-strand cDNAs were synthesized using the PrimeScript™ II 1st Strand cDNA Synthesis Kit (TaKaRa, Japan) for cloning cDNA sequences and the PrimeScript™ RT Master Mix (Perfect Real Time) (TaKaRa, Japan) for quantitative Real-Time PCR (qRT-PCR), respectively. Then the cDNA stored at -20 °C until used.

2.3. Cloning the full-length cDNA and genomic DNA of *CaMyD88* and *CaTRAF6*

The cDNA derived from healthy spleen was used as the template to clone the cDNA sequences. Partial sequences amplification, 5' and 3' rapid amplification of cDNA ends (RACE), and purification, cloning, and sequencing of PCR products were performed according to the methods in our previous research [22]. The degenerate primers, gene-specific primers, and adapter primers were listed in Table S1A. Partial sequences, 5'- and 3'-fragments with overlap were assembled to obtain the full-length cDNA of *CaMyD88* and *CaTRAF6*.

To obtain the genomic DNA sequences of *CaMyD88* and *CaTRAF6*, PCR was carried out using the primers (Table S1B) based on the obtained cDNA sequences, and genomic DNA isolated in section 2.2 was used as template. The PCR products were purified, cloned, and sequenced as described in Zhang et al. [21]. The obtained genomic sequences of *CaMyD88* and *CaTRAF6* were aligned with the cDNA sequences to identify the genomic structures of these two genes.

2.4. Bioinformatics

BLAST algorithm (<http://blast.ncbi.nlm.nih.gov/Blast.cgi>) was used to search homologous sequences. Multiple sequence alignments were performed using the DNAMAN 8.0 software. MEGA 6.0 was used to construct the neighbor-joining phylogenetic trees based on the deduced amino acid sequences and the bootstrap value was set to 1000 replicates to assess reliability. EXPASY (<http://web.expasy.org/translate/>) was used to translate the deduced amino acid sequences. Compute pI/Mw (http://web.expasy.org/compute_pi/) was used to calculate the theoretical isoelectric point (pI) and molecular weight (Mw) of the deduced amino acid. The protein domains were predicted by SMART program (<http://smart.embl-heidelberg.de>) and the three dimensional structure was constructed using the Swiss-Model (<http://swissmodel.expasy.org/>) and analyzed by the software SPDBV 4.01 and POV-Ray v3.6.

2.5. Quantitative Real-Time PCR

Samples collected in section 2.1 were used to investigate the tissue distribution, expression levels during embryonic development, and transcription responses in different tissues after challenges, respectively. The cDNA obtained in section 2.2 were diluted five times using EASY Dilution (for Real Time PCR) (TaKaRa, Japan) and then used as the templates for qRT-PCR. Gene-specific primers were designed based on the partial cDNA sequences in the present study and listed in Table S1C, and β -actin was used as the internal control. The qRT-PCR was performed using AceQ® qPCR SYBR® Green Master Mix (Vazyme, China) according to the manufacturer's protocol with the LightCycler 96 Real Time PCR System (Roche, Switzerland). Each sample was detected in triplicate.

2.6. Statistical analysis

The relative expression levels of target genes to reference gene were analyzed using the $2^{-\Delta\Delta Ct}$ method and presented as fold changes for the calibrator [24]. All data were expressed as mean \pm standard deviation ($n = 3$), and the statistical differences was assessed using one-way analysis of variance (ANOVA) implemented in software Microsoft Excel 2010. The significant level was set as $p = 0.05$.

3. Results

3.1. cDNA and genomic DNA sequences of *CaMyD88* and *CaTRAF6*

Full-length cDNA of *CaMyD88* (GenBank accession number: MK246404) was 2463 bp, including a 191 bp 5'-untranslated region (UTR), a 1417 bp 3'-UTR including five mRNA instability motifs (attta), and an 855 bp open reading frame (ORF) encoding for a putative protein with 284 amino acids, with an estimated Mw of 33.1 kD and a theoretical pI of 5.53 (Fig. S1A). Deduced amino acid sequence were analyzed using SMART program, and the result indicated that *CaMyD88* possessed the characteristic N-terminal death domain and C-terminal TIR domain (Fig. S1B). As shown in Fig. 1A, the 3D model of death domain consisted of α -helices and coils, while the TIR domain consisted of six β -sheets surrounded by six α -helices that formed a global fold. Five conserved amino acid residues (Arg184, Asp185, Lys205, Gln270, and Arg276) involved in signal transduction were found in the TIR domain and located on the spherical surface. Multiple sequences alignment revealed that the death domain contained three conserved amino acids (Trp70, Leu81, and Leu85) which were

associated to activate NF- κ B promoter (Fig. S2). The TIR domain of *CaMyD88* also harbored three conserved regions: box 1 (F/YDA), box 2 (RD-PG), and box 3 (a conserved W surrounded by basic residues) (Fig. S2). Genomic DNA sequence of *CaMyD88* was aligned with the cDNA sequence, as shown in Fig. 2A. The *CaMyD88* gene was comprised of five exons interrupted by four introns. The exon showed the same size (304, 123, 181, 92, and 155 bp for exon 1 to 5, respectively) in cyprinid fish, particularly, the size of fourth and fifth exon was absolutely consistent among the reported fish from GenBank database. However, the intron sizes were largely different in various fish species.

Full-length cDNA of *CaTRAF6* (GenBank accession number: MK246405) was identified to be 2555 bp, consisting of a 52 bp 5'-UTR, an 871 bp 3'-UTR including four mRNA instability motifs (attta), and a 1632 bp ORF encoding a protein of 543 amino acids with an estimated Mw of 61.7 kD and a theoretical pI of 5.81 (Fig. S3A). SMART analysis showed that *CaTRAF6* contained five domains including one N-terminal RING-type zinc finger domain, two TRAF-type zinc finger domains, one coiled-coil region (CCR), and one conserved C-terminal meprin and TRAF homology (MATH) domain (Fig. S3B). Using Swiss-Model online software, as shown in Fig. 1B, *CaTRAF6* was found to have the similar 3D model with that in human [25,26]. The coding sequence of *CaTRAF6* consisted of six exons and five introns as similar as that in common carp and zebrafish, while it contained seven exons and six introns in rock bream and orange-spotted grouper (Fig. 2B). Although two types of genomic structures were found in these fish species, the exon 2 to 5 in coding sequence showed the same length (151, 159, 72, and 78 bp, respectively) in all analyzed *TRAF6* (Fig. 2B).

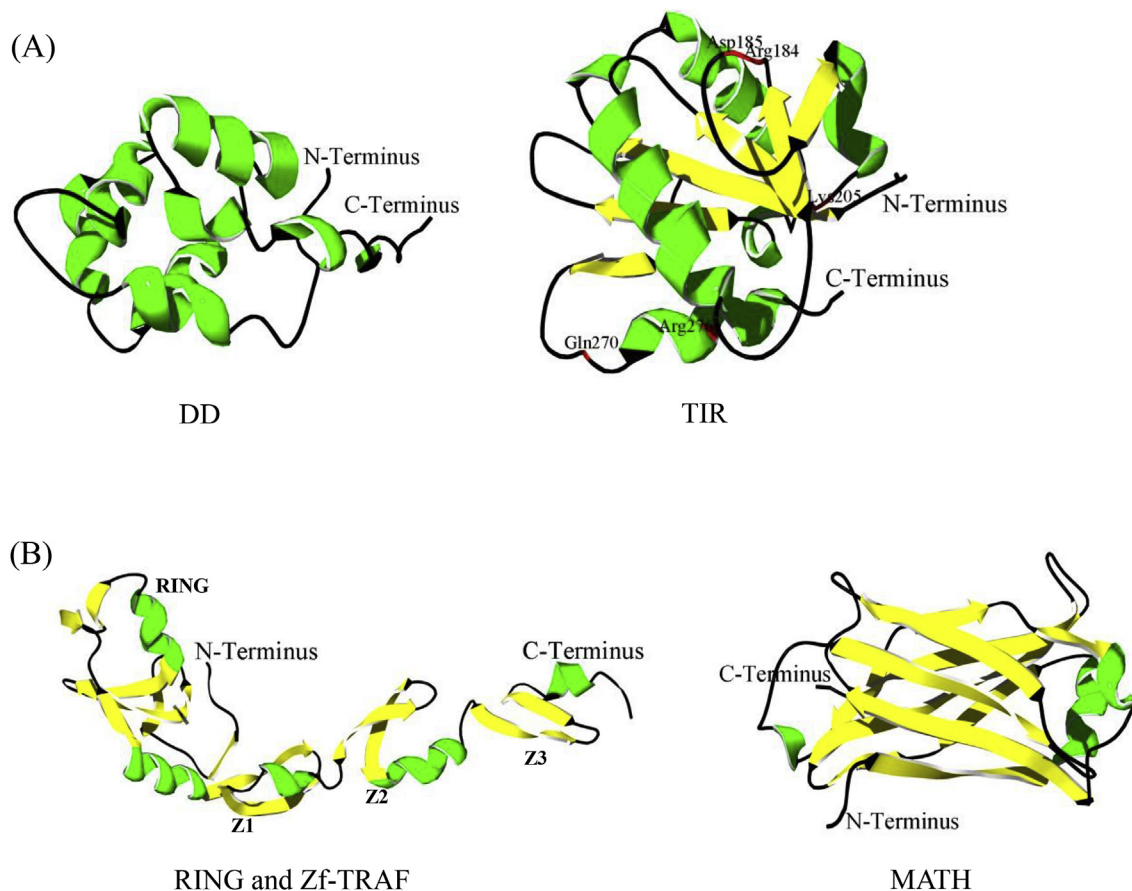
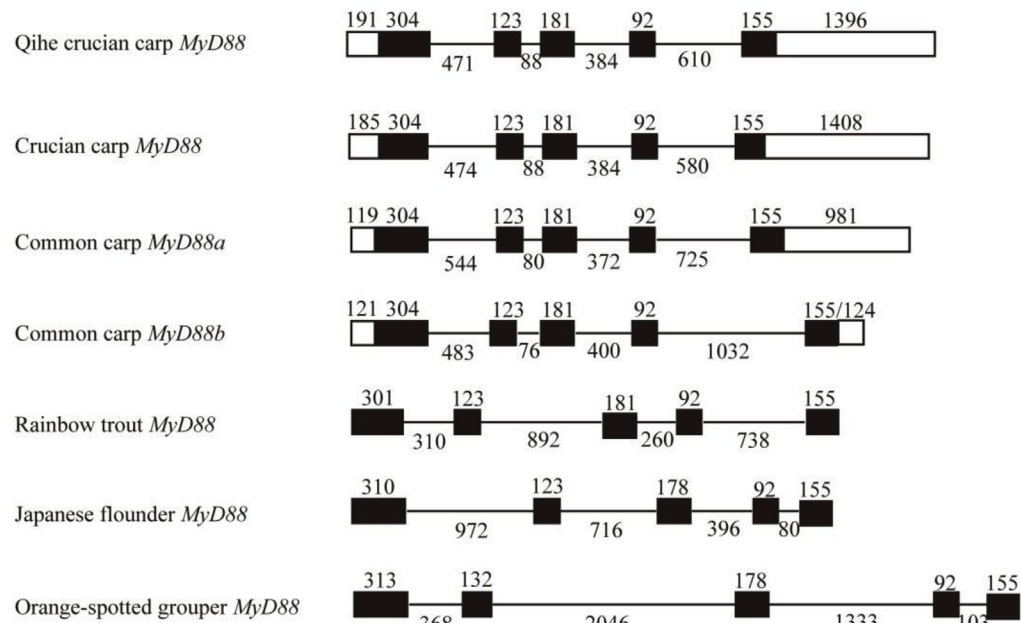


Fig. 1. The 3D model of *CaMyD88* (A) and *CaTRAF6* (B). The α -helices, β -sheets, and coils are shown in green, yellow, and black, respectively. Conserved amino acid residues in *CaMyD88* TIR domain are shown in red. Z1-Z3 in *TRAF6* indicates the zinc fingers as illustrated in human counterpart [25]. (For interpretation of the references to color in this figure legend, the reader is referred to the Web version of this article.)

(A)



(B)

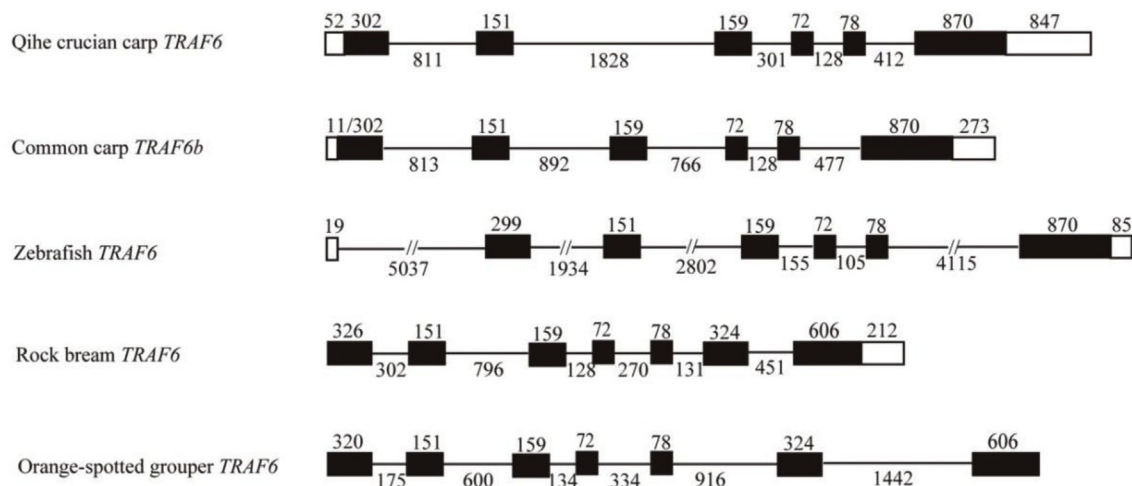


Fig. 2. Comparison of genomic structure of *MyD88* (A) and *TRAF6* (B) in various fish species. Exons are indicated with boxes (untranslated regions with white boxes and translated regions with black boxes) and introns with horizontal lines. The numbers showing the length (bp) of exons and introns are marked above and below the corresponding elements, respectively. Accession numbers of DNA sequences used in this figure are as follows: Crucian carp *MyD88*, [KF317670.1](#); Common carp *MyD88a*, [GU321986.2](#); Common carp *MyD88b*, [GU321987.2](#); Rainbow trout *MyD88*, [HG325726.1](#); Japanese flounder *MyD88*, [AB221347.1](#); Orange-spotted grouper *MyD88*, [JF271883.1](#); Common carp *TRAF6b*, [HM535646.1](#); Zebrafish *TRAF6*, [ENSDARG00000028058](#); Rock bream *TRAF6*, [KM034912.1](#); Orange-spotted grouper *TRAF6*, [KF137656.1](#).

3.2. Homology alignment and phylogenetic analysis

To determine the similarities and identities of CaMyD88/CaTRAF6 among different species, homology alignment of the deduced protein sequences was analyzed respectively. As shown in Table 1A, CaMyD88 showed the relatively high similarity (95.1–98.6%) and identity (90.5–96.5%) with that in Cyprinid fish. With other fish species, the similarity and identity of CaMyD88 were 79.3–84.6% and 69.0–75.5%, respectively. And CaMyD88 shared similarity (70.9%, 71.3%) and identity (59.5%, 58.1%) with that from human and mouse, respectively. With regard to CaTRAF6, it exhibited the highest similarity

(98.2%) and identity (96.1%) to common carp TRAF6b, whereas the similarity and identity of CaTRAF6 to other fish species was 72.2–97.2% and 61.1–94.7%, respectively. And it also exhibited similarity (68.4%, 68.2%) and identity (55.5%, 55.1%) respectively to human and mouse (Table 1B).

To reveal the evolutionary relationship for CaMyD88/CaTRAF6 among different species, phylogenetic trees were constructed based on full-length amino acid sequences. As shown in Fig. 3A, the phylogenetic tree constructed based on MyD88 was clustered into two branches: one for mammals and the other for bony fish, and the bony fish were further classified into two subgroups: freshwater fish and marine fish.

Table 1

Comparisons of the deduced amino acid sequences of CaMyD88 or CaTRAF6 with those from other species (BioEdit Sequence Alignment Editor).

Species	Accession number	Similarity (%)	Identity (%)
(A) CaMyD88			
Crucian carp MyD88	AGO57937.1	98.6	96.5
Zebrafish MyD88	NP_997979.2	97.5	91.2
Blunt snout bream MyD88	AKC45380.1	96.5	93.0
Common carp MyD88	ADQ08685.1	95.1	90.5
Channel catfish MyD88	NP_001187207.1	84.6	75.5
Ayu MyD88	BAI68386.1	84.3	74.6
Rainbow trout MyD88	CDG03206.1	84.2	72.6
Atlantic salmon MyD88	ABV59003.1	84.2	71.2
Japanese flounder MyD88	BAE94195.1	80.8	69.6
Turbot MyD88	AKM49934.1	80.1	69.6
Fugu MyD88	NP_001106666.1	79.6	68.9
Orange-spotted grouper MyD88	ADZ53063.1	79.3	69.0
Mouse MyD88	AAC53013.1	71.3	58.1
Human MyD88	AAC50954.1	70.9	59.5
(B) CaTRAF6			
Common carp TRAF6b	ADM45855.1	98.2	96.1
Common carp TRAF6a	ADF56651.2	97.2	94.7
Blunt snout bream TRAF6	AKC45381.1	95.6	91.7
Grass carp TRAF6	AGI51678.1	95.4	91.3
Zebrafish TRAF6	NP_001038217.1	93.2	86.7
Ayu TRAF6	BAI68388.1	75.4	65.9
Large yellow croaker TRAF6	XP_019128980.2	74.0	63.0
Orange-spotted grouper TRAF6	AGQ45557.1	74.0	63.0
Greasy grouper TRAF6	AHN13885.1	74.0	63.0
Japanese flounder TRAF6	AJE25833.1	72.2	61.1
Human TRAF6	NP_665802.1	68.4	55.5
Mouse TRAF6	BAA12705.1	68.2	55.1

Additionally, all Cyprinid fish were grouped into one cluster. The phylogenetic tree constructed based on TRAF6, as shown in Fig. 3B, was similar with phylogenetic relationship based on MyD88.

3.3. CaMyD88 and CaTRAF6 gene expression during development process of embryo and larva

Both CaMyD88 and CaTRAF6 were ubiquitously expressed during the developmental stages of embryos and larva (Fig. 4) and appeared to be developmentally regulated. As shown in Fig. 4A, the highest expression level of CaMyD88 was detected in fertilized eggs, followed by continually decreased level, and reached the lowest level at tail-bud, heart-beating, and hatching stages. After hatching, the mRNA expression of CaMyD88 was gradually increased from 1 dph to 10 dph followed by a slight decline at 20 dph but not significant ($p > 0.05$), and then elevated steeply at 30 dph. However, it was still lower than that in fertilized eggs at this last stage we studied (0.376-fold, $p < 0.05$). The expression level of CaTRAF6 was also the highest in fertilized eggs similar as CaMyD88, and then it was decreased sharply at cleavage stage (0.350-fold, $p < 0.05$). Thereafter, mRNA expression level was gradually decreased until hatching stage, although a slight but not significant ($p > 0.05$) increasing was observed at blastula stage. Subsequently, it was significantly elevated ($p < 0.05$) at 5 dph, about 4-fold compared with 1 dph. After this stage, no significant increase was found at the later stages. The expression level was only 0.14-fold compared with that in fertilized eggs until 30 dph, the last stage we studied (Fig. 4B).

3.4. CaMyD88 and CaTRAF6 gene expressions in different tissues

Quantitative RT-PCR was performed to respectively detect the mRNA expression levels of CaMyD88 and CaTRAF6 gene in various tissues. As shown in Fig. 5, CaMyD88 and CaTRAF6 showed a broadly expression distribution in the examined eleven tissues but the transcript level varied considerably among the different tissues. The highest expression of CaMyD88 was detected in the spleen (5.372-fold) followed by the liver, blood, muscle, head kidney, trunk kidney, and gill, and the lowest expression was observed in skin (Fig. 5A). The expression of CaTRAF6 was significantly higher in muscle (6.787-fold) and blood (4.202-fold) than in other tissues, and moderate in spleen, trunk kidney, head kidney, skin, and intestine, and the lowest in gill (Fig. 5B).

3.5. CaMyD88 and CaTRAF6 expression profiles in response to polyI:C, flagellin, and A. hydrophila challenges

The expression profiles of CaMyD88 were different in four tissues after polyI:C, flagellin, and A. hydrophila challenges (Fig. 6). In gill, compared with the control, CaMyD88 expression was up-regulated significantly but not much at 6 h post infection with polyI:C (1.575-fold, $p < 0.05$), 6 h and 24 h post infection with flagellin (1.564-fold and 1.634-fold, respectively, $p < 0.05$). However, it was down-regulated significantly ($p < 0.05$) at all the time points after fish were challenged by A. hydrophila and the minimum value was observed at 12 hpi (0.180-fold, $p < 0.05$) (Fig. 6A). In liver, the highest expression level was found at 24 h post infection with polyI:C and flagellin (5.457-fold and 6.768-fold, respectively) and significantly up-regulated compared with the control ($p < 0.05$), while it was down-regulated at 12 hpi and 24 hpi in A. hydrophila treated fish (about 0.2-fold, $p < 0.05$) and up-regulated at other time points (Fig. 6B). In spleen, the CaMyD88 expression was increased and then declined in fish treated by polyI:C and flagellin, and the peak value also appeared at 24 hpi, then decreased at 48 hpi and was significantly lower than that in the control ($p < 0.05$) (Fig. 6C). Meanwhile, compared with the control, it was down-regulated significantly at 3 h post infection with A. hydrophila followed by increasing dramatically at 6 hpi (2.679-fold, $p < 0.05$) and declined steeply at 12 hpi (0.287-fold, $p < 0.05$) (Fig. 6C). The CaMyD88 expression in head kidney increased at first and then decreased, the highest value appeared at 24 h post infection with polyI:C (2.677-fold, $p < 0.05$), flagellin (1.472-fold, $p > 0.05$), and A. hydrophila (3.78-fold, $p < 0.05$) (Fig. 6D).

In general, the CaTRAF6 expression was elevated early and then decreased to the basal level (Fig. 7). However, similar as CaMyD88, the expression of CaTRAF6 in gill of fish treated by A. hydrophila was also significantly down-regulated compared with the control (Fig. 7A). In liver, the highest level was detected at 24 h post infection with polyI:C (2.532-fold, $p < 0.05$), 24 h post infection with flagellin (8.004-fold, $p < 0.05$), and 6 h post infection with A. hydrophila (5.676-fold, $p < 0.05$), respectively (Fig. 7B). The peak value of CaTRAF6 expression in spleen of fish stimulated with polyI:C, flagellin, and A. hydrophila was significantly higher than that in the control and respectively observed at 24 hpi (3.002-fold, $p < 0.05$), 6 hpi (2.335-fold, $p < 0.05$), and 6 hpi (3.748-fold, $p < 0.05$), whereas no significant change was found at other time points (Fig. 7C). In head kidney, CaTRAF6 expression levels respectively touched peak value at 24 h post infection with polyI:C (2.140-fold), 12 h post infection with flagellin (2.343-fold), and 24 h post infection with A. hydrophila (2.948-fold), which were significantly higher than that in the control ($p < 0.05$) (Fig. 7D).

4. Discussion

MyD88 and TRAF6 were two crucial factors in the TLR signaling pathway. In the present study, MyD88 and TRAF6 were cloned and identified in Qihe crucian carp, and the full length cDNA sequence was 2463 bp and 2555 bp, respectively. The protein structure, homology

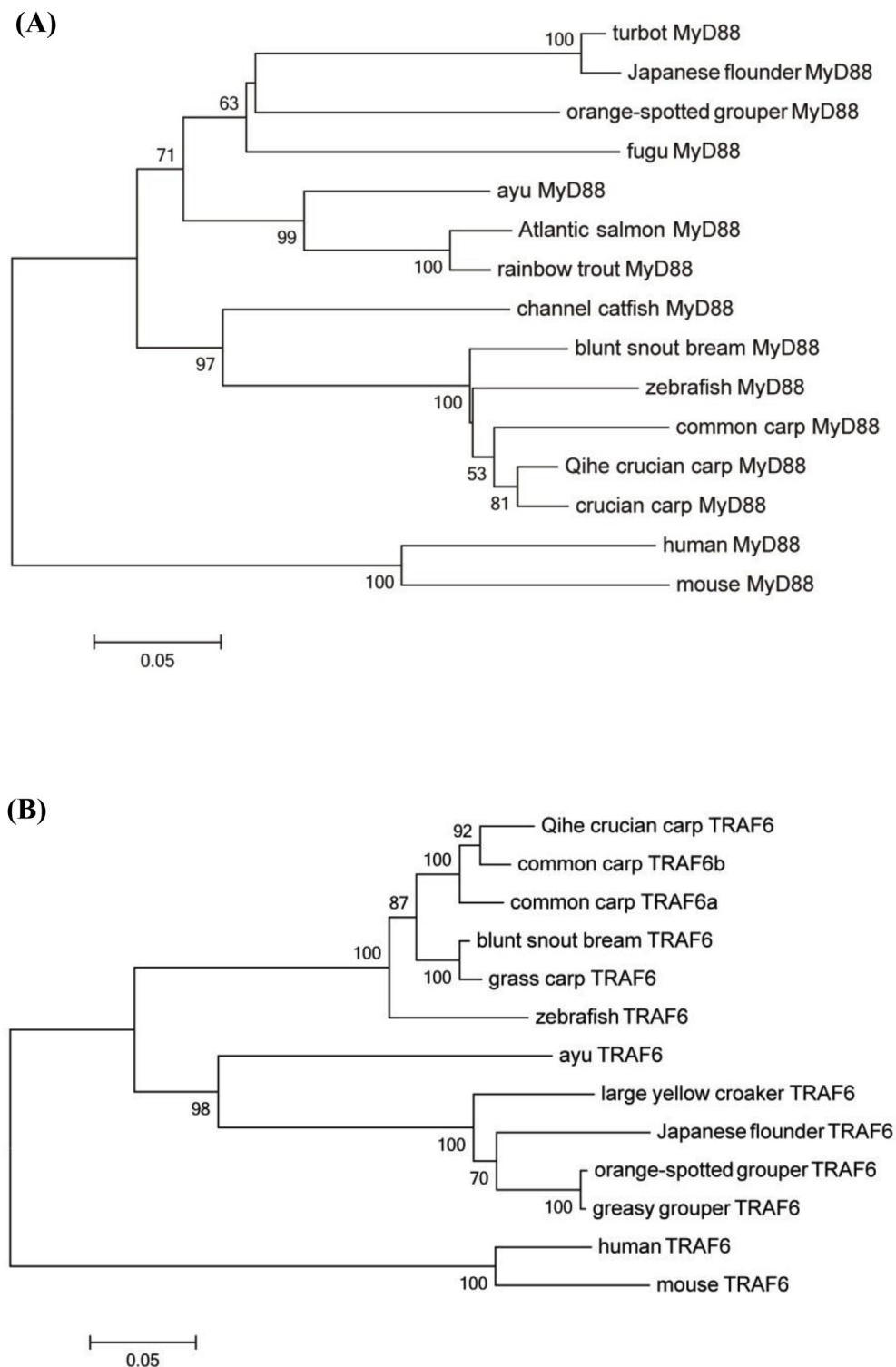


Fig. 3. Phylogenetic tree constructed based on CaMyD88 (A) or CaTRAF6 (B). Based on full-length amino acid sequences, the phylogenetic trees were constructed according to the neighbor-joining method using the Poisson correction model with MEGA6.0. All positions containing gaps and missing data were eliminated from the dataset (pairwise deletion). The numbers at the branches indicate bootstrap values. The GenBank accession numbers of sequences used to build the tree are shown in Table 1.

alignment and phylogenetic analysis based on the deduced amino acid indicated that the identified genes from Qihe crucian carp are indeed the homologue of *MyD88* and *TRAF6* in other species, and termed as *CaMyD88* and *CaTRAF6*.

As a crucial adaptor molecule, MyD88 plays an important role in

TLR signaling pathway. Our results showed that the CaMyD88 had the death domain and TIR domain as its orthologs in other fish species and mammals. Several conserved amino acid residues were found in CaMyD88, such as Trp70, Leu81, and Leu85 in death domain and Arg184, Asp185, Lys205, Gln270, and Arg276 in TIR domain. In

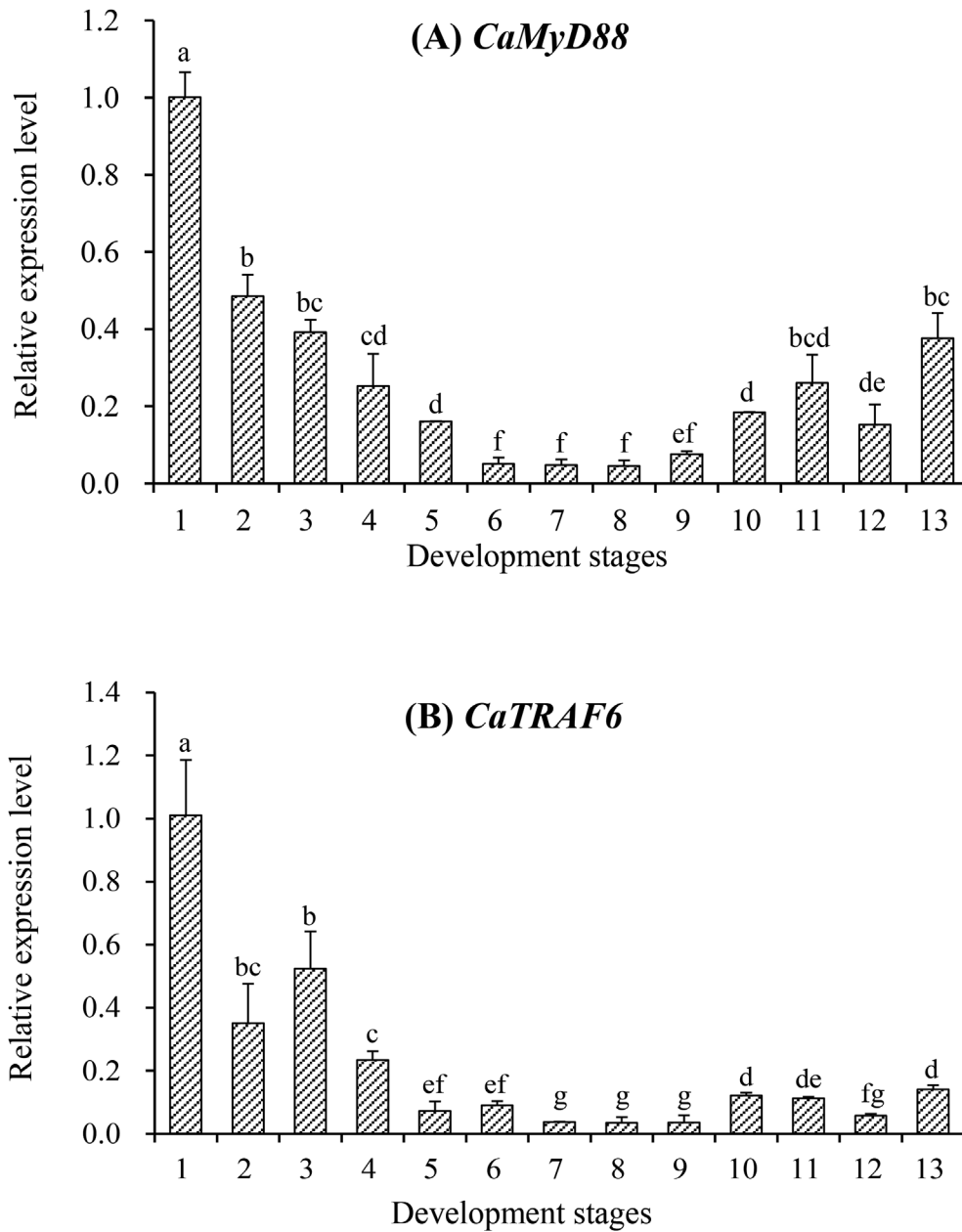


Fig. 4. Expression analysis of *CaMyD88* and *CaTRAF6* during development stages. 1: fertilized egg; 2: cleavage; 3: blastula; 4: gastrula; 5: neurula; 6: tail-bud; 7: heart-beating; 8: hatching; 9: 1 day post-hatched (dph); 10: 5 dph; 11: 10dph; 12: 20 dph; 13: 30 dph. The mRNA expression levels of target genes relative to β -actin were analyzed using the $2^{-\Delta\Delta Ct}$ method and gene expression in fertilized eggs was chosen as calibrator (set as 1). The relative expression of *CaMyD88* (A) and *CaTRAF6* (B) were presented as fold change for the calibrator. All data were expressed as mean \pm standard deviation (n = 3). Different letters above the bars indicate significant difference ($p < 0.05$).

Japanese eel, mutation of three conserved amino acids in death domain were modestly impaired the ability to activate NF- κ B promoter, suggesting their importance in signaling transduction [17]. The five conserved amino acid residues in TIR domain were involved in the interaction between human MyD88 and Mal in TLR4 signaling pathway [27]. In addition, three conserved boxes (boxes 1, 2 and 3) were also present in TIR domain of *CaMyD88*, and it has been suggested that the interaction with its cognate domains located in the cytoplasmic tails of activated TLRs or IL-1R was primarily depended on box 1, while the formation of loop structure that probably regulates downstream elements was depended on box 2 and the controlling trafficking and localization of the receptors in IL-1R family was depended on box 3, respectively [28–30]. Taken together, *MyD88* maybe share similar functions with that in mammalian and other fish species.

TRAFs family, consist of seven members (TRAF1-7), regulated the immune and inflammatory through transmission of signal which came from cell surface receptors [31]. Among these seven members, TRAF6 emerged earlier than other during evolution and was the core molecule in several immune receptors signaling pathways such as TLRs and IL-1R

[32,33]. In mammals, TRAF6 contained a RING-type zinc finger domain, five TRAF-type zinc finger domains, a CCR, and a conserved MATH domain [34]. In the present study, *CaTRAF6* was identified and also contained these four types of conserved domains, together with high level similarity and identity between sequences of TRAF6 in fishes and mammals, these results implied that they perform similar functions possibly. However, *CaTRAF6* only contained two TRAF-type zinc finger domains as well as in other piscine TRAF6s such as greasy grouper (*Epinephelus tauvina*) [35], rock bream (*Oplegnathus fasciatus*) [36], and Nile tilapia (*Oreochromis niloticus*) [37]. Whether the reduction in the number of TRAF-type zinc finger domains has effect on the function of TRAF6 is still unclear.

Gene evolution and role could be partly understood based on its genomic organization [36]. In the present study, the genomic structures of *CaMyD88* and *CaTRAF6* were identified. The exons of *MyD88* showed very similar sizes among the reported fish from GenBank database, while their intron sizes were largely different in various fish species. With regard to *TRAF6*, in spite of the appearance of two types of genomic structures, the exon 2 to 5 in coding sequence showed the

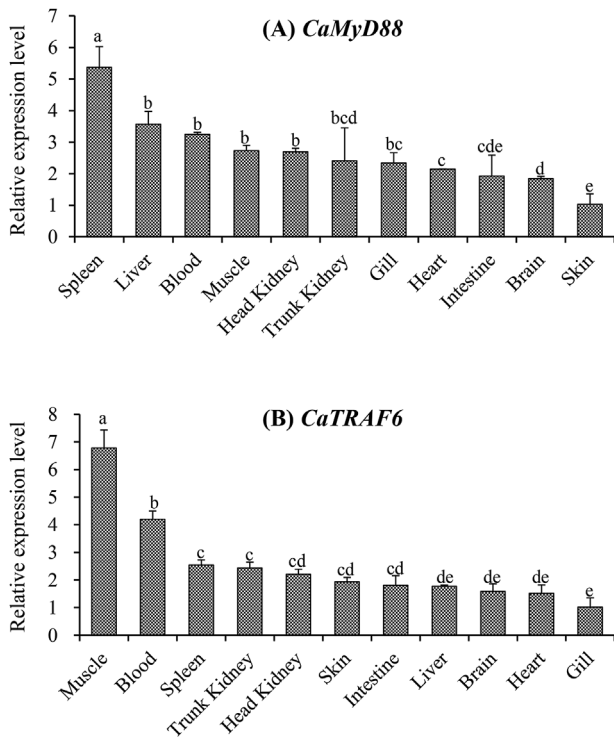


Fig. 5. Expression analysis of *CaMyD88* and *CaTRAF6* in different tissues. The mRNA expression levels of target genes relative to β -actin were analyzed using the $2^{-\Delta\Delta Ct}$ method. For the gene *CaMyD88* (A), the expression level in skin was chosen as calibrator (set as 1), and for the gene *CaTRAF6* (B), the expression level in gill was set as 1. The relative expressions of *CaMyD88* and *CaTRAF6* were presented as fold change for the calibrator. All data were expressed as mean \pm standard deviation (n = 3). Different letters above the bars indicate significant difference ($p < 0.05$).

same size in *TRAF6*. Conservation of exons indicated that *CaMyD88* (or *CaTRAF6*) could share the similar function with those in other fish species, and the variations of the intron sizes among different fish might imply the information of genetic evolution.

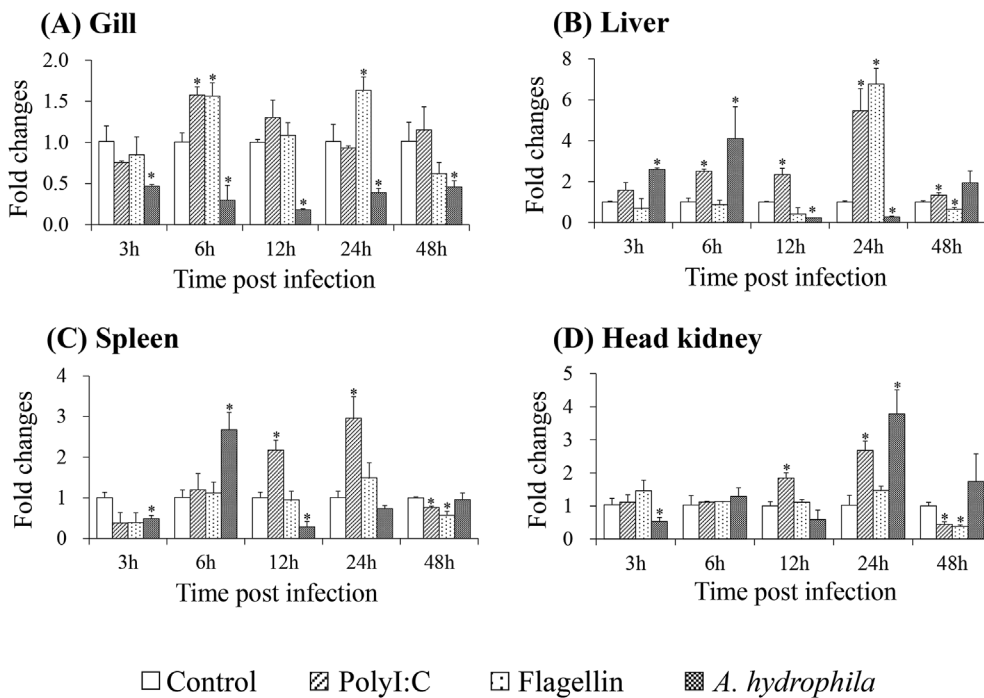


Fig. 6. Expression profiles of *CaMyD88* in gill (A), liver (B), spleen (C), and head kidney (D) at different time points after challenges. The mRNA expression levels of genes relative to β -actin were analyzed using the $2^{-\Delta\Delta Ct}$ method. The gene expression level in the control at the same time point was chosen as calibrator (set as 1). The relative expression of gene was presented as fold change relative to the calibrator. All data were expressed as mean \pm standard deviation (n = 3). Significant differences in the expression between the infected and control groups at the same time point were indicated with * ($p < 0.05$).

The expression patterns of *CaMyD88* and *CaTRAF6* in the developmental embryos and larva indicated that they were maternal genes, as the highest expression levels were detected in fertilized eggs. The existence of maternal mRNA have been reported in other fish species, e.g., *MyD88* and *TRAF6* in mrigal (*Cirrhinus mrigala*) were detected in various embryonic developmental stages and higher expression level of zebrafish *MyD88* was detected as early as the 4-cell stage [38,39]. Presence of maternal mRNA indicated that TLR signaling pathway including *MyD88* and *TRAF6* may play an important role in immune defense during ontogenic early stage. Consistent with this finding, our previous research suggested that *CaTLR5* and *CaTLR22* were constitutively expressed throughout the developmental stages and appeared to be developmentally regulated [22]. Similar with *MyD88* in zebrafish and *TRAF6* in mrigal [38,39], reductions of *CaMyD88* and *CaTRAF6* expressions after fertilization maybe result from consumption of maternal mRNA, and the increase after hatching maybe result from the up-regulation expression of these two genes at the later stages. Whatever, the lower expression level appeared at hatching stage implied that the immunity of embryos was very weak, and intensive care was needed to protect embryos from pathogens infection at this stage. However, *MyD88* in mrigal was almost stably expressed in all developmental stages from 0 h to 20 h after fertilization [38]. In addition, *TRAF6* expression pattern during development of half-smooth tongue sole (*Cynoglossus semilaevis*) was different from our study [40]. The expression difference was observed in different fish species, and further studies are required for confirmation.

With regard to mRNA expression in various tissues, *CaMyD88* and *CaTRAF6* were broadly expressed in all examined tissues, although tissue specific differences appeared among the different tissues. The extensive expressions of *MyD88* or *TRAF6* were also detected in other fish species such as silvery pomfret [18], rainbow trout (*Oncorhynchus mykiss*) [41], and Nile tilapia [37]. These results implied that these two genes may be important in the immune surveillance system in various tissues of the host. However, the expression profiles were different in several fish species. For example, *MyD88* in Qihe crucian carp, silvery pomfret [18], and turbot (*Scophthalmus maximus*) [42] showed the highest expression level in spleen, liver, and heart, respectively. The expression of *TRAF6* in rainbow trout was most abundant in liver and lowest in skin [41]. In Nile tilapia, the highest expression of *TRAF6* was

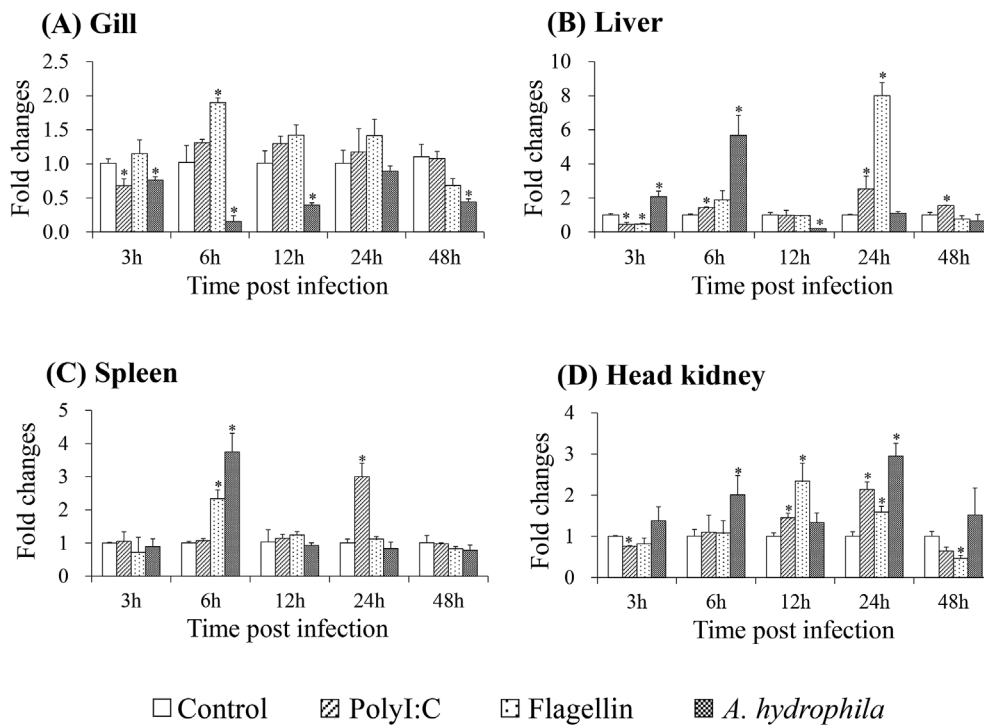


Fig. 7. Expression profiles of *CaTRAF6* in gill (A), liver (B), spleen (C), and head kidney (D) at different time points after challenges. The mRNA expression levels of genes relative to β -actin were analyzed using the $2^{-\Delta\Delta Ct}$ method. The gene expression level in the control at the same time point was chosen as calibrator (set as 1). The relative expression of gene was presented as fold change relative to the calibrator. All data were expressed as mean \pm standard deviation ($n = 3$). Significant differences in the expression between the infected and control groups at the same time point were indicated with * ($p < 0.05$).

found in spleen and lowest in head-kidney [37]. In the present study, *CaTRAF6* was significantly higher expressed in muscle and blood than other tissues, and lowest in gill. The differences of mRNA expression profiles among the various tissues may result from the variations of fish species, development stages, and genetic background. *MyD88* and *TRAF6* were highly expressed in non-immune tissues such as liver and muscle may imply that these two genes have other functions besides the critical role in immune system.

MyD88 and *TRAF6* were important signal transducers in TLRs pathway, linked upstream TLRs and downstream elements, and activated the signaling cascade, which resulted in the production of pro-inflammatory cytokines finally to eliminate the pathogens [5]. In the present study, mRNA expressions of *CaMyD88* and *CaTRAF6* were mostly up-regulated after stimulation in spite of down-regulation sometimes appeared at some time points or in some tissues. This result was supported by several previous studies in other fish species which showed the responses of *MyD88* and *TRAF6* to challenges by bacterial, virus, or their PAMPs. In Japanese eel, mRNA expression of *MyD88* reached the peak value at 24 h post infection with polyI:C in head kidney, spleen, and liver [17]. In liver, spleen, and kidney of blunt snout bream infected with *A. hydrophila*, *MyD88* and *TRAF6* expression was up-regulated at the early stage and then returned to normal level or even below at the late stage [16]. The mRNA expression of *TRAF6* was up-regulated in liver, spleen, head kidney, and gill of rock bream administered with flagellin [36]. In together, these research results mentioned above indicated that *MyD88* and *TRAF6* were involved in immune defense of host against pathogenic invasion. However, mRNA expression of *CaMyD88* and *CaTRAF6* was down-regulated significantly in gill of fish treated by *A. hydrophila*, and this finding was in agreement with the results of the previous studies in mrigal and black carp. In mrigal, the expressions of *MyD88* and *TRAF6* were down-regulated in gill, liver, and kidney after infected with *A. hydrophila* or *Edwardsiella tarda* [38]. LPS stimulation led to the obvious decrease of black carp *TRAF6* transcription in *Mylopharyngodon piceus* fin (MPF) cells [19]. Unfortunately, the mechanism of down-regulation of gene expression in challenged fish was still unclear. Research in mouse demonstrated the existence of an intricate regulatory network of cross-talk of the TLR2, TLR4, and TLR5 pathways in intestinal epithelial cells. Activations of

TLR2 and TLR4 could weaken the responses of TLR5 signaling [43]. This negative feedback mechanism also occurred in human [44]. Future study should be performed to determine whether fish *MyD88* and *TRAF6* in TLR signal pathway were down-regulated by a similar mechanism. Interestingly, *TRAF6* expression was detected to find two peak values in Nile tilapia stimulated by formalin-inactivated *Streptococcus agalactiae* or polyI:C [37], and it was proposed that *TRAF6* plays an important role in innate immunity, sometimes in adaptive immune. This finding was not found in the present study. With respect to the role of *TRAF6* in adaptive immune, the more studies need to be performed to confirm this viewpoint.

In conclusion, the full-length cDNA and genomic DNA of *CaMyD88* and *CaTRAF6* were successfully achieved in Qihe crucian carp in the present study. Protein structure of *CaMyD88* and *CaTRAF6* respectively contained the typical domains as in other fish species. The characteristic analysis of *CaMyD88* and *CaTRAF6* showed the high conservation with their homologues in mammals and other fish species. Both *CaMyD88* and *CaTRAF6* were ubiquitously expressed throughout the embryonic development with the obvious change, and in various tissues with tissue specificity. In addition, both *CaMyD88* and *CaTRAF6* indicated the significant responses to stimulation by polyI:C, flagellin, and *A. hydrophila*. Therefore, it was suggested that *CaMyD88* and *CaTRAF6* play an important role in immune response and immune defense in Qihe crucian carp.

Acknowledgments

This work was funded by the Joint Fund of Natural Science Foundation of China and Natural Science Foundation of Henan Province (U1604104), the Henan Province Innovative Research Team in Science and Technology (201706081), the Key Scientific Research Project in University of Henan Province (18A240003), the Excellent Young Scholars Fund of Henan Normal University (YQ201706), and the Science Foundation for Young Scientists of Henan Normal University (2016QK22). We would like to thank our colleagues for the valuable suggestions on the overall manuscript preparation.

Appendix A. Supplementary data

Supplementary data to this article can be found online at <https://doi.org/10.1016/j.fsi.2019.02.034>.

References

- P.R. Rauta, M. Samanta, H.R. Dash, B. Nayaka, S. Das, Toll-like receptors (TLRs) in aquatic animals: Signaling pathways, expressions and immune responses, *Immunol. Lett.* 158 (2014) 14–24 [http://doi.org/10.1016/j.imlet.2013.11.013](https://doi.org/10.1016/j.imlet.2013.11.013).
- C.A. Janeway, R. Medzhitov, Innate immune recognition, *Annu. Rev. Immunol.* 20 (2002) 197–216 [http://doi.org/10.1109/37.60419](https://doi.org/10.1109/37.60419).
- O. Takeuchi, S. Akira, Pattern recognition receptors and inflammation, *Cell* 140 (2010) 805–820 [http://doi.org/10.1016/j.cell.2010.01.022](https://doi.org/10.1016/j.cell.2010.01.022).
- L.Y. Zhu, L. Nie, G. Zhu, L.X. Xiang, J.Z. Shao, Advances in research of fish immune-relevant genes: A comparative overview of innate and adaptive immunity in teleosts, *Dev. Comp. Immunol.* 39 (2013) 39–62 [http://doi.org/10.1016/j.dci.2012.04.001](https://doi.org/10.1016/j.dci.2012.04.001).
- J. Zhang, X.H. Kong, C.J. Zhou, L. Li, G.X. Nie, X.J. Li, Toll-like receptor recognition of bacteria in fish: Ligand specificity and signal pathways, *Fish Shellfish Immunol.* 41 (2014) 380–388 [http://doi.org/10.1016/j.fsi.2014.09.022](https://doi.org/10.1016/j.fsi.2014.09.022).
- Z. Kanwal, G.F. Wiegertjes, W.J. Veneman, A.H. Meijer, H.P. Spaik, Comparative studies of Toll-like receptor signalling using zebrafish, *Dev. Comp. Immunol.* 46 (2014) 35–52 [http://doi.org/10.1016/j.dci.2014.02.003](https://doi.org/10.1016/j.dci.2014.02.003).
- H. Wesche, W.J. Henzel, W. Shillinglaw, S. Li, Z. Cao, MyD88: An adapter that recruits IRAK to the IL-1 receptor complex, *Immunity* 7 (1997) 837–847 [http://doi.org/10.1016/S1074-7613\(00\)80402-1](https://doi.org/10.1016/S1074-7613(00)80402-1).
- T. Kawai, S. Akira, The role of pattern-recognition receptors in innate immunity: update on Toll-like receptors, *Nat. Immunol.* 11 (2010) 373–384 [http://doi.org/10.1038/ni.1863](https://doi.org/10.1038/ni.1863).
- J.Y. Chung, Y.C. Park, H. Ye, H. Wu, All TRAFs are not created equal: common and distinct molecular mechanisms of TRAF-mediated signal transduction, *J. Cell Sci.* 115 (2002) 679–688 [http://doi.org/10.1101/gad.213002](https://doi.org/10.1101/gad.213002).
- T. Kobayashi, M.C. Walsh, Y. Choi, The role of TRAF6 in signal transduction and the immune response, *Microb. Infect.* 6 (2004) 1333–1338 [http://doi.org/10.1016/j.micinf.2004.09.001](https://doi.org/10.1016/j.micinf.2004.09.001).
- Y.W. Li, X.C. Luo, X.M. Dan, X.Z. Huang, W. Qiao, Z.P. Zhong, et al., Orange-spotted grouper (*Epinephelus coioides*) TLR2, MyD88 and IL-1 β involved in anti-*Cryptocaryon irritans* response, *Fish Shellfish Immunol.* 30 (2011) 1230–1240 [http://doi.org/10.1016/j.fsi.2011.04.012](https://doi.org/10.1016/j.fsi.2011.04.012).
- Y.W. Li, X. Li, X.X. Xiao, F. Zhao, X.C. Luo, X.M. Dan, et al., Molecular characterization and functional analysis of TRAF6 in orange-spotted grouper (*Epinephelus coioides*), *Dev. Comp. Immunol.* 44 (2014) 217–225 [http://doi.org/10.1016/j.dci.2013.12.011](https://doi.org/10.1016/j.dci.2013.12.011).
- P. Kongchum, E.M. Hallerman, G. Hulata, L. David, Y. Palti, Molecular cloning, characterization and expression analysis of TLR9, MyD88 and TRAF6 genes in common carp (*Cyprinus carpio*), *Fish Shellfish Immunol.* 30 (2011) 361–371 [http://doi.org/10.1016/j.fsi.2010.11.012](https://doi.org/10.1016/j.fsi.2010.11.012).
- J. Su, J. Dong, T. Huang, R. Zhang, C. Yang, J. Heng, Myeloid differentiation factor 88 gene is involved in antiviral immunity in grass carp *Ctenopharyngodon idella*, *J. Fish. Biol.* 78 (2011) 973–979 [http://doi.org/10.1111/j.1095-8649.2011.02910.x](https://doi.org/10.1111/j.1095-8649.2011.02910.x).
- F. Zhao, Y.W. Li, H.J. Pan, S.Q. Wu, C.B. Shi, X.C. Luo, et al., Grass carp (*Ctenopharyngodon idella*) TRAF6 and TAK1: molecular cloning and expression analysis after *Ichthyophthirius multifiliis* infection, *Fish Shellfish Immunol.* 34 (2013) 1514–1523 [http://doi.org/10.1016/j.fsi.2013.03.003](https://doi.org/10.1016/j.fsi.2013.03.003).
- N.T. Tran, H. Liu, J. Ivan, W.M. Wang, Blunt snout bream (*megalobrama amblycephala*) Myd88 and TRAF6: characterisation, comparative homology modelling and expression, *Int. J. Mol. Sci.* 16 (2015) 7077–7097 [http://doi.org/10.3390/ijms16047077](https://doi.org/10.3390/ijms16047077).
- W.S. Huang, Z.X. Wang, Y. Liang, P. Nie, B. Huang, Characterization of MyD88 in Japanese eel, *Anguilla japonica*, *Fish Shellfish Immunol.* 81 (2018) 374–382 [http://doi.org/10.1016/j.fsi.2018.07.028](https://doi.org/10.1016/j.fsi.2018.07.028).
- Q.X. Gao, F. Yin, C.J. Zhang, Y.F. Yue, P. Sun, M.H. Min, et al., Cloning, characterization, and function of MyD88 in silvery pomfret (*Pampus argenteus*) in response to bacterial challenge, *Int. J. Biol. Macromol.* 103 (2017) 327–337 [http://doi.org/10.1016/j.ijbiomac.2017.05.039](https://doi.org/10.1016/j.ijbiomac.2017.05.039).
- S. Jiang, J. Xiao, J. Li, H. Chen, C.Y. Wang, C.L. Feng, et al., Characterization of the black carp TRAF6 signaling molecule in innate immune defense, *Fish Shellfish Immunol.* 67 (2017) 147–158 [http://doi.org/10.1016/j.fsi.2017.06.011](https://doi.org/10.1016/j.fsi.2017.06.011).
- C.J. Zhou, B.H. Li, L.Y. Ma, Y.J. Zhao, X.H. Kong, The complete mitogenome of natural triploid *Carassius auratus* in Qihe River, Mitochondrial DNA 27 (2016) 605–606 [http://doi.org/10.3109/19401736.2014.908367](https://doi.org/10.3109/19401736.2014.908367).
- J. Zhang, L. Li, X.H. Kong, F. Wu, C.J. Zhou, G.X. Nie, et al., Expression patterns of Toll-like receptors in natural triploid *Carassius auratus* after infection with *Aeromonas hydrophila*, *Vet. Immunol. Immunopathol.* 168 (2015) 77–82 [http://doi.org/10.1016/j.vetimm.2015.08.009](https://doi.org/10.1016/j.vetimm.2015.08.009).
- J. Zhang, L. Wang, Y.J. Zhao, X.H. Kong, F. Wu, X.L. Zhao, Molecular characterization and expression analysis of toll-like receptors 5 and 22 from natural triploid *Carassius auratus*, *Fish Shellfish Immunol.* 64 (2017) 1–13 [http://doi.org/10.1016/j.fsi.2017.03.004](https://doi.org/10.1016/j.fsi.2017.03.004).
- J. Sambrook, D.W. Russell, *Molecular Cloning*, fourth ed., Cold Spring Harbor Laboratory Press, New York, 2006.
- K.J. Livak, T.D. Schmittgen, Analysis of relative gene expression data using real-time quantitative PCR and the 2^{- $\Delta\Delta C_T$} method, *Methods* 25 (2001) 402–408 [http://doi.org/10.1006/meth.2001.1262](https://doi.org/10.1006/meth.2001.1262).
- Q. Yin, S.C. Lin, B. Lamothe, M. Lu, Y.C. Lo, G. Hura, et al., E2 interaction and dimerization in the crystal structure of TRAF6, 16, *Nat. Struct. Mol. Biol.* 16 (2009) 658–666 [http://doi.org/10.1038/nsmb.1605](https://doi.org/10.1038/nsmb.1605).
- H. Ye, J.R. Arron, B. Lamothe, M. Cirilli, T. Kobayashi, N.K. Shevde, et al., Distinct molecular mechanism for initiating TRAF6 signalling, *Nature* 418 (2002) 443–447 [http://doi.org/10.1038/nature00888](https://doi.org/10.1038/nature00888).
- H. Ohnishi, H. Tochio, Z. Kato, K.E. Orii, A. Li, T. Kimura, et al., Structural basis for the multiple interactions of the MyD88 TIR domain in TLR4 signaling, *Proc. Natl. Acad. Sci. U. S. A.* 106 (2009) 10260–10265 [http://doi.org/10.1073/pnas.0812956106](https://doi.org/10.1073/pnas.0812956106).
- Y. Xu, X. Tao, B. Shen, T. Horn, R. Medzhitov, J.L. Manley, et al., Structural basis for signal transduction by the Toll/interleukin-1 receptor domains, *Nature* 408 (2000) 111–115 [http://doi.org/10.1038/35040600](https://doi.org/10.1038/35040600).
- T. Takano, H. Kondo, I. Hirono, T. Saito-Taki, M. Endo, T. Aoki, Identification and characterization of a myeloid differentiation factor 88 (MyD88) cDNA and gene in Japanese flounder, *Paralichthys olivaceus*, *Dev. Comp. Immunol.* 30 (2006) 807–816 [http://doi.org/10.1016/j.dci.2005.11.003](https://doi.org/10.1016/j.dci.2005.11.003).
- J.L. Slack, K. Schooley, T.P. Bonnett, J.L. Mitcham, E.E. Qvarnstrom, J.E. Sims, et al., Identification of two major sites in the type I interleukin-1 receptor cytoplasmic region responsible for coupling to pro-inflammatory signaling pathways, *J. Biol. Chem.* 275 (2000) 4670–4678 [http://doi.org/10.1074/jbc.275.7.4670](https://doi.org/10.1074/jbc.275.7.4670).
- J. Inoue, T. Ishida, N. Tsukamoto, N. Kobayashi, A. Naito, S. Azuma, et al., Tumor necrosis factor receptor-associated factor (TRAF) family: adapter proteins that mediate cytokine signaling, *Exp. Cell Res.* 254 (2000) 14–24 [http://doi.org/10.1006/excr.1999.4733](https://doi.org/10.1006/excr.1999.4733).
- A. Grech, R. Quinn, D. Srinivasan, X. Badoux, R. Brink, Complete structural characterisation of the mammalian and Drosophila TRAF genes: implications for TRAF evolution and the role of RING finger splice variants, *Mol. Immunol.* 37 (2000) 721–734 [http://doi.org/10.1016/S0161-5890\(00\)00098-5](https://doi.org/10.1016/S0161-5890(00)00098-5).
- Z. Cao, J. Xiong, M. Takeuchi, T. Kurama, D.V. Goeddel, TRAF6 is a signal transducer for interleukin-1, *Nature* 383 (1996) 443–446 [http://doi.org/10.1038/383443a0](https://doi.org/10.1038/383443a0).
- T. Ishida, S. Mizushima, S. Azuma, N. Kobayashi, T. Tojo, K. Suzuki, et al., Identification of TRAF6, a novel tumor necrosis factor receptor-associated factor protein that mediates signaling from an amino-terminal domain of the CD40 cytoplasmic region, *J. Biol. Chem.* 271 (1996) 28745–28748 [http://doi.org/10.1074/jbc.271.46.28745](https://doi.org/10.1074/jbc.271.46.28745).
- J.G. Wei, M.L. Guo, P. Gao, H.S. Ji, P.F. Li, Y. Yan, et al., Isolation and characterization of tumor necrosis factor receptor-associated factor 6 (TRAF6) from grouper, *Epinephelus taivina*, *Fish Shellfish Immunol.* 39 (2014) 61–68 [http://doi.org/10.1016/j.fsi.2014.04.022](https://doi.org/10.1016/j.fsi.2014.04.022).
- N. Umashanthan, S. Bathige, K.S. Revathy, B.H. Nam, C.Y. Choi, J. Lee, Molecular genomic-and transcriptional-aspects of a teleost TRAF6 homolog: possible involvement in immune responses of *Oplegnathus fasciatus* against pathogens, *Fish Shellfish Immunol.* 42 (2015) 66–78 [http://doi.org/10.1016/j.fsi.2014.10.022](https://doi.org/10.1016/j.fsi.2014.10.022).
- Z.W. Wang, Y. Huang, Y. Li, B. Wang, Y.S. Lu, L.Q. Xia, et al., Biological characterization, expression, and functional analysis of tumor necrosis factor receptor-associated factor 6 in Nile tilapia (*Oreochromis niloticus*), *Fish Shellfish Immunol.* 80 (2018) 497–504 [http://doi.org/10.1016/j.fsi.2018.06.036](https://doi.org/10.1016/j.fsi.2018.06.036).
- M. Basu, B. Swain, N.K. Maiti, P. Routray, M. Samanta, Inductive expression of toll-like receptor 5 (TLR5) and associated downstream signaling molecules following ligand exposure and bacterial infection in the Indian major carp, mrigal (*Cirrhinus mrigala*), *Fish Shellfish Immunol.* 32 (2012) 121–131 [http://doi.org/10.1016/j.fsi.2011.10.031](https://doi.org/10.1016/j.fsi.2011.10.031).
- A.M. van der Sar, O.W. Stockhammer, C. van der Laan, H.P. Spaik, W. Bitter, A.H. Meijer, MyD88 innate immune function in a zebrafish embryo infection model, *Infect. Immun.* 74 (2006) 2436–2441 [http://doi.org/10.1128/IAI.74.4.2436-2441.2006](https://doi.org/10.1128/IAI.74.4.2436-2441.2006).
- Y. Chen, L. Fan, T.T. Liu, Y.Z. Liu, Z. Li, Q.Q. Zhang, Molecular cloning and expression analysis of TRAF6 and TAK1 in half-smooth tongue sole (*Cynoglossus semilaevis*), *J. Fish. Sci. China* 22 (2015) 867–876 [http://doi.org/10.3724/SP.J.1118.2015.15082](https://doi.org/10.3724/SP.J.1118.2015.15082).
- J.H. Jang, H. Kim, J.H. Cho, Molecular cloning and functional characterization of TRAF6 and TAK1 in rainbow trout, *Oncorhynchus mykiss*, *Fish Shellfish Immunol.* 84 (2019) 927–936 <https://doi.org/10.1016/j.fsi.2018.11.002>.
- J.Y. Lin, G.B. Hu, C.H. Yu, S. Li, Q.M. Liu, S.C. Zhang, Molecular cloning and expression studies of the adapter molecule myeloid differentiation factor 88 (MyD88) in turbot (*Scophthalmus maximus*), *Dev. Comp. Immunol.* 52 (2015) 166–171 [http://doi.org/10.1016/j.dci.2015.05.013](https://doi.org/10.1016/j.dci.2015.05.013).
- R.A.M.H. van Aubel, A.M. Keestra, D.J.E.B. Krooshoop, W. van Eden, J.P.M. van Putten, Ligand-induced differential cross-regulation of Toll-like receptors 2, 4 and 5 in intestinal epithelial cells, *Mol. Immunol.* 44 (2007) 3702–3714 [http://doi.org/10.1016/j.molimm.2007.04.001](https://doi.org/10.1016/j.molimm.2007.04.001).
- E.S. Cabral, H. Gelderblom, R.L. Hornung, P.J. Munson, R. Martin, A.R. Marques, Borrelia burgdorferi Lipoprotein-Mediated TLR2 Stimulation Causes the Down-Regulation of TLR5 in Human Monocytes, *J. Infect. Dis.* 193 (2006) 849–859 [http://doi.org/10.1086/500467](https://doi.org/10.1086/500467).